

## MODELING OF HEAT AND MASS TRANSFER IN A HYDROCARBON FLUID UNDER INDUCTIVE HEATING

L. A. Kovaleva,<sup>1</sup> V. N. Kireev,<sup>2</sup>  
and A. A. Musin<sup>1</sup>

UDC 532.516.5

*Results of numerical simulations of the thermal action on a high-viscosity hydrocarbon fluid with temperature-dependent viscosity and thermal conductivity are presented. A system of equations of thermal convection in the Boussinesq approximation is used as the constitutive equations to describe the convection of the hydrocarbon fluid. The dynamics of the temperature field and convective structures in the fluid is studied. The spatial motion of the fluid is found to be locally nonuniform; the motion is accompanied by vortex flows; as a result, two regions with significantly different temperatures are formed in the medium.*

**Key words:** *inductive heating, hydrocarbon fluid, thermal convection, heat transfer, mathematical model.*

**Introduction.** Results of experimental research of heating of heavy hydrocarbon systems by an inductive heater and results of mathematical modeling of this experiment were reported in [1]. The thermal convection of the fluid was taken into account by introducing an effective thermal conductivity. The fluid under study was a heavy hydrocarbon system, which has extremely low values of fluidity and thermal conductivity at low temperatures. Based on results of experimental and numerical studies, a conclusion was drawn that the effective thermal conductivity became substantially increased with increasing temperature, which was a consequence of the emergence of local spots of vortex motion of the fluid in regions where the temperature exceeded some threshold value corresponding to the beginning of fluidity. The spatial region where this motion occurred and the temperature field in this region displayed permanent irregular changes, which was observed visually and was recorded by temperature gauges located inside the reservoir. A mathematical model of heating of a heavy hydrocarbon system in a closed reservoir is proposed in the paper to describe the effects noted above. The model takes into account not only the effect of temperature on viscosity and thermal conductivity of the fluid, but also the presence of free convective motion of the fluid.

**Mathematical Model.** We consider a closed metallic reservoir whose base is covered by a concrete layer, and there is an inductor tube in the center. The space between the inductor tube and the outer wall of the reservoir is filled by a high-viscosity hydrocarbon fluid. Some part of the inductor tube wall is heated by the inductor tube; as a result, the fluid becomes heated. The computational domain corresponding to the physical model described above is schematically shown in Fig. 1. The problem is solved in an axisymmetric formulation in a cylindrical coordinate system with the origin in the center of the reservoir base and with the  $z$  axis directed upward, perpendicular to the base. From the viewpoint of mathematical modeling, the physical model is a multilayer system consisting of the inductor tube, concrete layer, and hydrocarbon medium (see Fig. 1). The temperature field is calculated in each layer; the velocity field of the convective flow of the fluid is additionally determined in the hydrocarbon medium.

---

<sup>1</sup>Bashkiriya State University, Ufa 450074. <sup>2</sup>Institute of Mechanics, Ufa Research Center, Russian Academy of Sciences, Ufa 450054; liana@ic.bashedu.ru; kireev@anrb.ru; mus-airat@yandex.ru. Translated from *Prikladnaya Mekhanika i Tekhnicheskaya Fizika*, Vol. 50, No. 1, pp. 95–100, January–February, 2009. Original article submitted January 29, 2008.

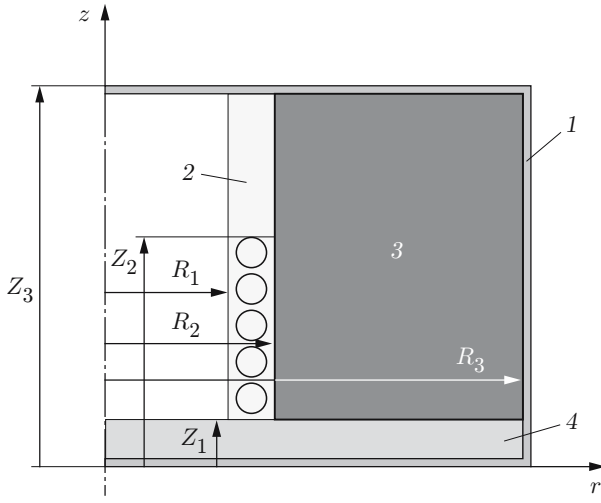


Fig. 1. Computational domain geometry: 1) metallic reservoir; 2) inductor tube; 3) hydrocarbon fluid; 4) concrete layer.

In the inductor tube wall, the heat generated by vortex flows initiated by the inductance coil is modeled by introducing internal distributed sources of heat. The equation of heat conduction in the inductor tube wall has the form

$$\rho_m c_m \frac{\partial T}{\partial t} = \frac{k_m}{r} \frac{\partial}{\partial r} \left( r \frac{\partial T}{\partial r} \right) + k_m \frac{\partial^2 T}{\partial z^2} + q, \quad R_1 < r \leq R_2, \quad Z_1 < z \leq Z_3, \quad (1)$$

where

$$q = \begin{cases} N_0 / [\pi(R_2^2 - R_1^2)l], & Z_1 < z \leq Z_2, \\ 0, & Z_2 < z \leq Z_3 \end{cases}$$

is the density of the distributed heat sources,  $\rho_m$ ,  $c_m$ , and  $k_m$  are the density, specific heat, and thermal conductivity of the metal,  $N_0$  is the inductor power,  $R_1$  and  $R_2$  are the inner and outer radii of the inductor tube,  $l$  is the inductor height,  $Z_1$  is the thickness of the concrete layer, and  $Z_2$  and  $Z_3$  are the distances from the reservoir base to the upper surface of the inductor and to the fluid surface, respectively.

The equation of heat conduction in the concrete layer is

$$\rho_b c_b \frac{\partial T}{\partial t} = \frac{k_b}{r} \frac{\partial}{\partial r} \left( r \frac{\partial T}{\partial r} \right) + k_b \frac{\partial^2 T}{\partial z^2}, \quad R_1 < r \leq R_3, \quad 0 \leq z \leq Z_1, \quad (2)$$

where  $\rho_b$ ,  $c_b$ , and  $k_b$  are the density, specific heat, and thermal conductivity of concrete;  $R_3$  is the reservoir radius.

Convective motion of the hydrocarbon fluid is described by a system of equations of heat convection in the Boussinesq linear approximation [2]:

$$\begin{aligned} \rho_f \left( \frac{\partial u}{\partial t} + \frac{1}{r} \frac{\partial}{\partial r} (ruu) + \frac{\partial}{\partial z} (vu) \right) &= -\frac{\partial P}{\partial r} + \frac{1}{r} \frac{\partial}{\partial r} \left( r\eta_f \frac{\partial u}{\partial r} \right) + \frac{\partial}{\partial z} \left( \eta_f \frac{\partial u}{\partial z} \right) - \eta_f \frac{u}{r^2}, \\ \rho_f \left( \frac{\partial v}{\partial t} + \frac{1}{r} \frac{\partial}{\partial r} (rvu) + \frac{\partial}{\partial z} (vv) \right) &= -\frac{\partial P}{\partial z} + \frac{1}{r} \frac{\partial}{\partial r} \left( r\eta_f \frac{\partial v}{\partial r} \right) + \frac{\partial}{\partial z} \left( \eta_f \frac{\partial v}{\partial z} \right) + \beta \rho_f g T, \\ \rho_f c_f \left( \frac{\partial T}{\partial t} + \frac{1}{r} \frac{\partial}{\partial r} (ruT) + \frac{\partial}{\partial z} (vT) \right) &= \frac{1}{r} \frac{\partial}{\partial r} \left( rk_f \frac{\partial T}{\partial r} \right) + \frac{\partial}{\partial z} \left( k_f \frac{\partial T}{\partial z} \right), \\ \frac{1}{r} \frac{\partial}{\partial r} (ru) + \frac{\partial v}{\partial z} &= 0, \quad R_2 < r \leq R_3, \quad Z_1 < z \leq Z_3. \end{aligned} \quad (3)$$

Here  $\rho_f$ ,  $\eta_f$ ,  $c_f$ , and  $k_f$  are the density, dynamic viscosity, specific heat, and thermal conductivity of the hydrocarbon fluid,  $u$  and  $v$  are the components of velocity of thermal motion of the fluid in the  $r$  and  $z$  directions, respectively,  $P$  is the pressure,  $\beta$  is the coefficient of thermal expansion of the fluid,  $g$  is the free-fall acceleration, and  $T$  is the temperature.

The thermal conductivity of the fluid is assumed to be a linear function of temperature [1]:

$$k_f(T) = k_{f0}[1 + b(T - T_0)]$$

( $k_{f0}$  is the thermal conductivity at a temperature  $T = T_0$  and  $b$  is the temperature coefficient of thermal conductivity). The viscosity of the hydrocarbon fluid also depends on temperature: we use the approximated dependence of viscosity on temperature in the form of two exponents, which was obtained on the basis of experimental data [1]:

$$\eta(T) = \begin{cases} \eta_{01} \exp(-\gamma_1(T - 35.5)), & 35.5^\circ\text{C} < T < 54.2^\circ\text{C}, \\ \eta_{02} \exp(-\gamma_2(T - 54.2)), & 54.2^\circ\text{C} < T < 75.0^\circ\text{C}. \end{cases}$$

Here  $\eta_{01} = 1460 \text{ Pa}\cdot\text{sec}$  is the viscosity of the hydrocarbon fluid at  $T = 35.5^\circ\text{C}$ ,  $\eta_{02} = 0.228 \text{ Pa}\cdot\text{sec}$  is the viscosity of the hydrocarbon fluid at  $T = 54.2^\circ\text{C}$ ,  $\gamma_1 = 0.497 \text{ K}^{-1}$  is the temperature coefficient at  $T = 35.5\text{--}54.2^\circ\text{C}$ , and  $\gamma_2 = 0.031 \text{ K}^{-1}$  is the temperature coefficient at  $T > 54.2^\circ\text{C}$ .

**Boundary Conditions.** At the initial time, the fluid is at rest, and the setup has a constant temperature equal to the ambient temperature:

$$u(r, z, 0) = v(r, z, 0) = 0, \quad T(r, z, 0) = T_0. \quad (4)$$

No-slip conditions are imposed for velocities on all solid walls:

$$u|_G = v|_G = 0 \quad (5)$$

(the subscript  $G$  refers to the inner boundaries of the reservoir). The outer surface of the reservoir is subjected to the condition of heat transfer with the ambient medium by the law of free convection in an unbounded space. The outer wall of the reservoir and its base are thermally insulated. The condition of heat exchange with air in a closed space is imposed on the inner surface of the inductor tube. The resultant boundary conditions have the form

$$\begin{aligned} \alpha_h(T(r, Z_3, t) - T_0) &= -k_m \frac{\partial T(r, Z_3, t)}{\partial z}, \\ \alpha_h(T(r, Z_3, t) - T_0) &= -k_f \frac{\partial T(r, Z_3, t)}{\partial z}, \\ \alpha_v(T(R_1, z, t) - T_0) &= -k_m \frac{\partial T(R_1, z, t)}{\partial r}, \\ \frac{\partial T(R_3, z, t)}{\partial r} &= 0, \quad \frac{\partial T(r, 0, t)}{\partial z} = 0, \end{aligned} \quad (6)$$

where  $\alpha_h$  and  $\alpha_v$  are the heat-transfer coefficients along the horizontal and vertical walls, respectively, and  $T_0$  is the initial temperature of the medium and the temperature of air surrounding the experimental setup. Identical temperatures and heat fluxes (boundary conditions of the fourth kind) are set on the remaining boundaries between the layers.

All equations and boundary conditions are brought to dimensionless form. The constitutive parameters are the Grashof number  $\text{Gr} = \beta g L^3 \theta / \mu_0^2$  and the Prandtl number  $\text{Pr} = \mu_0 / a$  [ $\theta$  is the characteristic difference in temperature,  $L$  is the characteristic size,  $\mu_0 = \eta / \rho$  is the kinematic viscosity, and  $a = k / (\rho c_p)$  is the thermal diffusivity]. The Grashof and Prandtl numbers determine the Biot number [3]:

$$\text{Bi} = \alpha L / k_a = f(\text{Gr}_a, \text{Pr}_a)$$

( $\alpha$  is the heat-transfer coefficient and  $k_a$  is the thermal conductivity of air; the subscript  $a$  refers to air).

The coefficient of heat transfer along the horizontal plane is determined from the equation [3]

$$\text{Bi} = 0.65(\text{Gr}_a \text{Pr}_a)^{1/4} (\text{Pr}_a / \text{Pr}_w)^{1/4},$$

where the subscript  $w$  refers to the wall. The heat-transfer coefficient in the annular gap is calculated by the formula [3]

$$\text{Bi} = 0.18(\text{Gr}_a \text{Pr}_a)^{1/4} (\text{Pr}_a / \text{Pr}_w)^{1/4}.$$

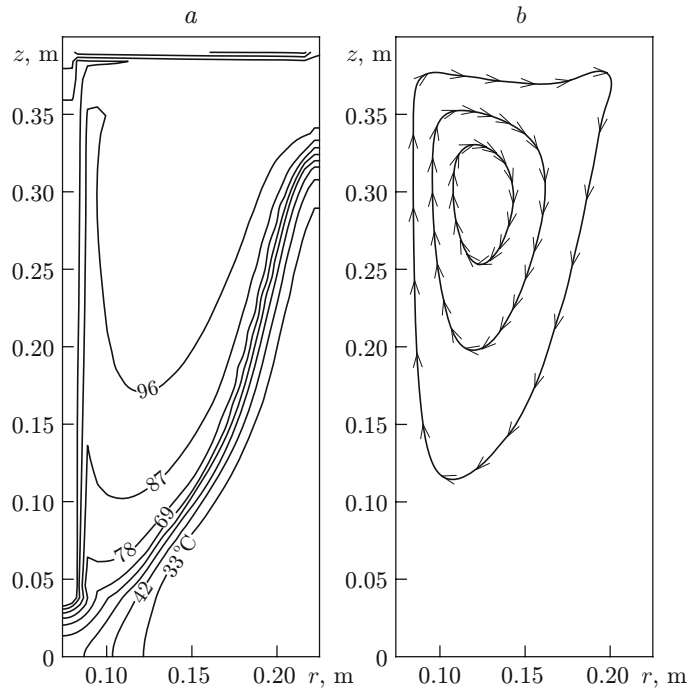


Fig. 2. Temperature field (a) and streamlines (b) at  $t = 150$  min.

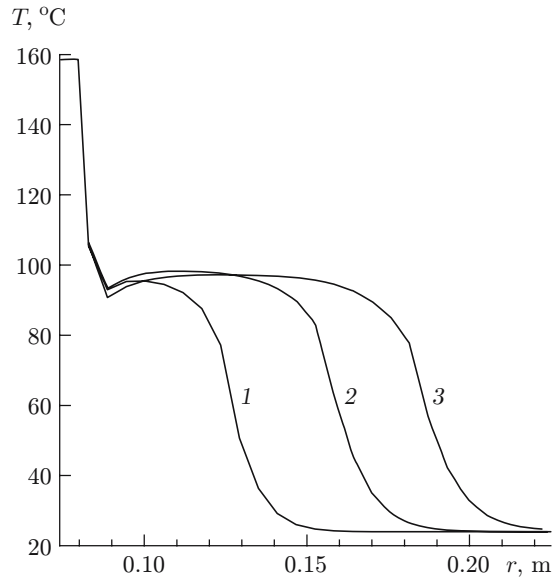


Fig. 3

Fig. 3. Temperature distributions in the central horizontal section of the reservoir at different times:  $t = 50$  (1),  $100$  (2), and  $150$  min (3).

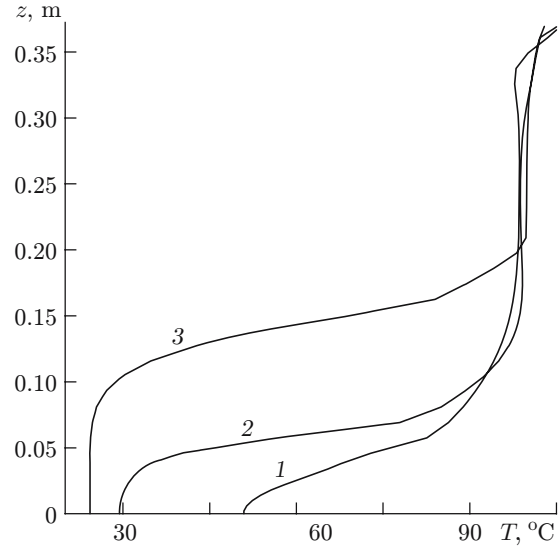


Fig. 4

Fig. 4. Temperature distributions in the vertical sections of the reservoir at different distances from the reservoir centerline:  $r = 0.10$  (1),  $0.15$  (2), and  $0.20$  m (3).

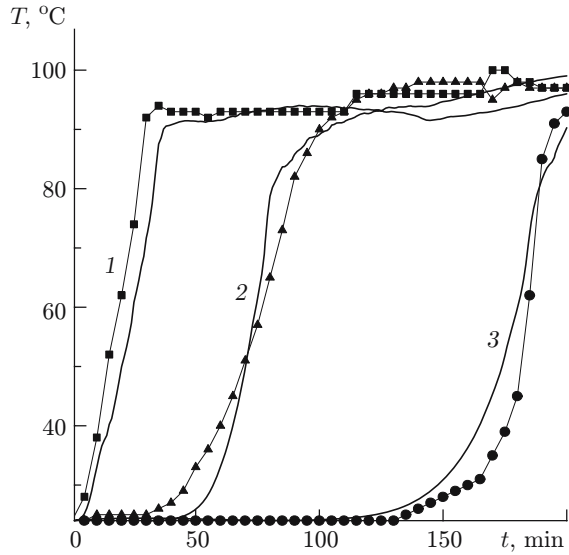


Fig. 5. Time evolution of the fluid temperature: the points 1, 2, and 3 are the experimental results obtained by the first, second, and third thermocouple, respectively; the curves are the corresponding calculations.

**Calculation Results.** System (1)–(3) with the boundary conditions (4)–(6) was solved numerically by a control-volume method with the use of the “Simple” algorithm [4]. The following values of the medium parameters and constants of the physical model were used in the calculations:  $k_f = 0.125 \text{ W}/(\text{m} \cdot \text{K})$ ,  $c_f = 1864 \text{ J}/(\text{kg} \cdot \text{K})$ ,  $\rho_f = 954 \text{ kg}/\text{m}^3$ ,  $k_m = 45 \text{ W}/(\text{m} \cdot \text{K})$ ,  $c_m = 461 \text{ J}/(\text{kg} \cdot \text{K})$ ,  $\rho_m = 7900 \text{ kg}/\text{m}^3$ ,  $k_b = 0.279 \text{ W}/(\text{m} \cdot \text{K})$ ,  $c_b \rho_b = 2.6 \cdot 10^6 \text{ J}/(\text{m}^3 \cdot \text{K})$ ,  $k_a = 0.02896 \text{ W}/(\text{m} \cdot \text{K})$ ,  $c_a \rho_a = 1065 \text{ J}/(\text{m}^3 \cdot \text{K})$ ,  $\mu_a = 1.897 \cdot 10^6 \text{ m}^2/\text{sec}$ ,  $Z_1 = 0.04 \text{ m}$ ,  $Z_2 = 0.29 \text{ m}$ ,  $Z_3 = 0.39 \text{ m}$ ,  $R_1 = 0.074 \text{ m}$ ,  $R_2 = 0.08 \text{ m}$ ,  $R_3 = 0.225 \text{ m}$ ,  $N_0 = 1224 \text{ W}$ , and  $T_0 = 24^\circ\text{C}$ .

A comparison of the results of simulations and experimental data shows that the best agreement is achieved for the following initially unknown parameters of the fluid:  $b = 0.0095 \text{ K}^{-1}$  and  $\beta = 2.1 \cdot 10^{-6} \text{ K}^{-1}$ .

The calculated results predict that the heat transfer in the fluid occurs only by the mechanism of molecular heat conduction for a rather long time after the beginning of inductive heating. The reason is the high viscosity of the fluid and its low fluidity at the initial time. As the fluid temperature increases, its viscosity decreases, and there arises a zone of convective flow in the upper part of the reservoir. Upward flows with rather high velocities (up to 4 mm/sec) develop near the hot wall of the inductor tube. Figure 2 shows the temperature field and the streamlines at the time  $t = 150 \text{ min}$  after the beginning of heating. It is seen that the region of intense convective mixing increases, but there also remains a “stagnant” region where the motion is absent.

The idea about the dynamics of propagation of the temperature front in the fluid can be derived from Fig. 3, which shows the temperature distribution in the central horizontal section of the reservoir at different times. The temperature drastically decreases in a thin boundary layer near the inductor tube wall, which is caused by the presence of a convective vortex flow near the inductor tube wall. This vortex flow entrains the heat inward the reservoir and favors the inflow of a colder fluid to the wall.

Figure 4 shows the temperature distributions in vertical sections at different distances from the reservoir centerline at different times. It follows from Fig. 4 that the temperature is almost identical in all sections in the upper part of the reservoir owing to intense convective mixing of the fluid, whereas significant temperature gradients are observed in the lower part.

Figure 5 shows the time evolution of the fluid temperature due to heating. The experimental data and calculated results are in good agreement.

This work was supported by the Russian Foundation for Basic Research (Grant No. 08-01-97032).

## REFERENCES

1. L. A. Kovaleva, N. M. Nasyrov, V. I. Maksimochkin, and R. R. Suf'yanov, "Experimental and numerical modeling of the thermal conductivity of high-viscosity hydrocarbon systems," *J. Appl. Mech. Tech. Phys.*, **46**, No. 6, 851–856 (2005).
2. G. Z. Gershuni and E. M. Zhukhovitskii, *Convective Stability of an Incompressible Fluid* [in Russian], Nauka, Moscow (1972).
3. A. V. Klimenko and V. M. Zorin (eds.), *Heat-Power Engineering and Heat Technology*, Book 2: *Theoretical Fundamentals of Heat Technology. Heat-Technology Experiment: Reference Book* [in Russian], Izd. Mosk. Énerg. Inst., Moscow (2001).
4. S. V. Patankar, *Numerical Heat Transfer and Fluid Flow*, Hemisphere–McGraw Hill, Washington–New York (1980).